An improved proportional control forgetting factor recursive least square-Monte Carlo adaptive extended Kalman filtering algorithm for high-precision state-of-charge estimation of lithium-ion batteries.

ZHU, C., WANG, S., YU, C., ZHOU, H. and FERNANDEZ, C.

2023

An improved proportional control forgetting factor recursive least square-Monte Carlo adaptive extended Kalman filtering algorithm for high-precision state-of-charge estimation of lithium-ion batteries

Chenyu Zhu[1] · Shunli Wang[1] · Chunmei Yu[1] · Heng Zhou[1] · Carlos Fernandez[2]

Corresponding author: Shunli Wang 497420789@qq.com

[1] School of Information Engineering, Southwest University of Science and Technology, Mianyang 621010, China

[2] School of Pharmacy and Life Sciences, Robert Gordon University, Aberdeen AB10-7GJ, UK

Abstract

For lithium-ion batteries, the state of charge (SOC) of batteries plays an important role in the battery management system, and the accuracy of the battery model and parameter identification is the basis of SOC estimation. Considering that the system has inevitable steady-state errors and the influence of random noise on SOC estimation results under dynamic conditions, this paper proposed an improved proportional control forgetting factor recursive least square-Monte Carlo adaptive extended Kalman filtering (PCFFRLS-MCAEKF) algorithm for high-precision state-of-charge estimation of lithium-ion batteries. The experimental results show that the proportional control forgetting factor recursive least square algorithm has higher parameter identification accuracy under HPPC and BBDST conditions. Under HPPC working conditions, the root mean square error of PCFFRLS-MCAEKF algorithm is reduced by 1.275%, 0.687%, and 0.549% compared with FFRLS- EKF, PCFFRLS-EKF, and PCFFRLS-AEKF algorithm, and the average absolute error is reduced by 0.71%, 0.537%, and 0.11%. Under BBDST working conditions, the SOC estimation result of PCFFRLS-MCAEKF algorithm is closer to the real SOC, which is consistent with the result obtained under HPPC working conditions. The experimental results show that under HPPC and BBDST working conditions, the PCFFRLS-MCAEKF algorithm can better improve the accuracy and robustness of SOC estimation than FFRLS-EKF, PCFFRLS-EKF, and PCFFRLS-AEKF algorithms.

Keywords Lithium-ion battery · State of charge · Monte Carlo · Adaptive extended Kalman filtering · Proportional control

Introduction

Because of the global warming caused by greenhouse gases and the urban heat island effect, reducing greenhouse gas emissions has become an important measure to protect the environment [1]. The traditional energy supply has been unable to meet the social and economic development and people's needs, and new energy battery technology is a powerful way to alleviate this problem [2]. To reduce the enormous pressure on the ecological environment caused by the emission of gases from traditional automobiles, new energy automobiles are gradually recognized by people, and battery technology is the key point of the development of new energy automobile technology [3]. The demand for power batteries is higher and higher, and the use of lithium-ion batteries is the most extensive.

There are many methods to estimate the state of charge of batteries, such as ampere-hour method, open-circuit voltage method [4], internal resistance method, discharge experiment method, neural network method, and Kalman filtering method. The ampere-hour method [5], also known as Coulomb counting method, is a small computational effort. It calculates the battery charge status only by using the integral link. It is the most commonly used method to estimate state of charge. This method considers the measured current as a cell, integrates it to get the released or absorbed power of the battery, and subtracts the integrated power from the initial power to get the state-of-charge value of the battery. Open-circuit voltage method is a common method to calculate battery state of charge [6]. Battery state of charge is estimated from the open-circuit voltage measured by the instrument when the battery is open. This method is more accurate than the time integral method, but the estimation time limit is more stringent than the time integral method, which requires that the battery be stationary for a longer time.

The principle of estimating the battery state of charge using the Kalman filtering algorithm [7] is the ampere-hour integration method. The voltage is measured by instruments or meters, and the calculation data of the former is corrected using a filtering method. The Kalman filtering is a tracking method based on real-time data. Using the Kalman filtering to estimate battery state of charge requires creating a suitable circuit model, which is more accurate than other methods and can better reflect the dynamic performance of the battery. The Kalman filter is only applicable to linear systems. When the system is nonlinear and can be approximated by linearization, the extended Kalman filter [8] is a good choice for state estimation, but its estimation results have large errors because the noise effects in the actual process are ignored. To reduce this error, an adaptive filtering method is added to the extended Kalman filtering algorithm. The adaptive extended Kalman filtering algorithm [9] estimates and corrects the process and measurement noise of the system by comparing the final estimates with the predictions. At the same time, process noise and measurement noise of the system is estimated and corrected, and average estimation and covariance are adjusted to reduce the impact of noise [10] on state-of-charge estimation, to obtain higher accuracy of state-of-charge estimation results. In recent years, many advanced SOC estimation methods have also emerged. For example, unscented Kalman filter (UKF), cubature Kalman filter (CKF), and BPNN algorithm optimized by artificial intelligence. The UKF algorithm avoids solving the Jacobian matrix [11], but its parameter selection problem has not been completely solved. The CKF algorithm overcomes the divergence or precision degradation of UKF in high-dimensional state space [12], but the estimation accuracy is not high due to the uncertainty of prior noise. BPNN [13] algorithm has poor estimation accuracy when dealing with dynamic current changes.

The state-of-charge estimation largely depends on the equivalent model [14] established for battery characteristics. To improve the accuracy of parameter identification of the battery models, it is necessary to adopt an appropriate parameter identification algorithm. The commonly used parameter identification methods can be divided into offline and online methods. The forgetting factor recursive least square algorithm [15–17] is a commonly used parameter identification method, which improves the data saturation problem of the recursive least square algorithm when identifying time-varying parameters.

The changing pattern of the output response of the control system after the end of the transition process is called the steady state. The steady-state error is the difference between the expected steady-state output and the actual steady-state output. The higher the steady-state error of the control system, the higher the control accuracy. This error cannot be completely eliminated, which can only be reduced by selecting high-precision components and improving the system gain value. The general parameter identification method does not consider the factors of system steady-state error, which leads to inaccurate parameter identification results. The accuracy of the model is determined by the error value between the real voltage and the real-time output voltage of the model. In this paper, considering the inevitable steady-state error, an improved proportional control forgetting factor recursive least squares algorithm is proposed to identify the parameters of the second- order RC equivalent circuit model. This algorithm improves the forgetting factor recursive least square algorithm and uses the proportional control forgetting factor recursive least square algorithm to identify the algorithm. The proportional control is added to the algorithm to reduce the steady-state error and improve the accuracy of model parameter identification. At the same time, use the Monte Carlo method to optimize the adaptive extended Kalman filtering algorithm to estimate the state of charge of lithium-ion batteries. This method reduces the effect of real noise by a large number of resampling, making the state-of-charge estimation more accurate and reliable. The estimation accuracy of the algorithm is further improved.

Mathematical analysis

Second-order RC model

When estimating the state of charge of lithium-ion batteries, it is necessary to establish an appropriate equivalent model. The most commonly used equivalent circuit model in engineering applications is simple in structure and can well reflect the battery characteristics [18]. The equivalent circuit models are mainly divided into the Pint model, the Thevenin model [19], and the second-order RC model. The Pint model has the simplest structure, but it often fails to reflect the battery characteristics [20]. Based on the Pint model, the Thevenin model considers more comprehensive factors and increases the polarization capacitance and resistance to better reflect the operating characteristics of batteries. The second-order RC model [21] can better reflect the battery characteristics, which reflects the ohm internal resistance of the battery through the resistance R_0, while the polarization reaction in the battery is represented by two RC parallel circuits. Therefore, the second-order RC model is selected according to the above judgment that is shown in Fig. 1.

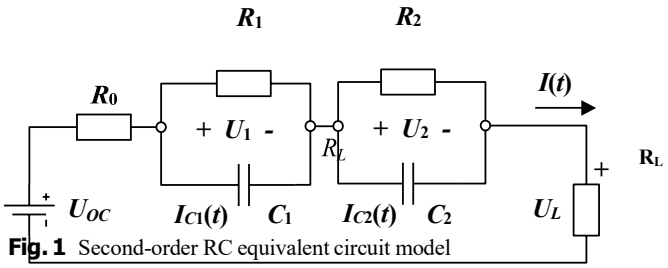

Fig. 1 Second-order RC equivalent circuit model

The parameters should be identified with the second- order RC model, including the ohmic internal resistance R_0, and the polarization resistance R_1 and R_2, the polarization capacitance C_1 and C_2. U_1 and U_2 are the voltage obtained when the resistance R_1 and R_2 current is I. U_{oc} is open circuit voltage, and U_L is output terminal voltage. The expressions for the voltage and current of the equivalent circuit obtained from the Kirchhoff voltage law are shown in Eq. (1).

$$\begin{cases} U_L = U_{oc} - U_0 - U_1 - U_2 \\ I = \dfrac{U_0}{R_0} = \dfrac{U_1}{R_1} + C_1\dfrac{dU_1}{dt} = \dfrac{U_2}{R_2} + C_2\dfrac{dU_2}{dt} \end{cases} \tag{1}$$

The output voltage and current can be obtained through the HPPC test [22]. Using the knowledge of modern control theory, the equivalent circuit model can be discretized [23]. The discrete state equation can be obtained as shown in Eq. (2).

$$SOC(k) = SOC(k_0) - \frac{\int_0^k I(k)\,\eta dk}{Q_0} \tag{2}$$

For lithium-ion batteries, the state of charge of the battery refers to the amount of electricity left in the battery at the current moment, which is an important part of the battery management system [24, 25]. The value of the battery state of charge is related to the charge–discharge times and charge–discharge current of the battery during use. The calculation is expressed numerically as the ratio of the remaining battery power to the rated capacity of the battery. Combined with the state-of-charge definition, the discrete state-space equation can be obtained as shown in Eq. (3).

$$\begin{bmatrix} SOC_{k+\Delta k} \\ U_{1,k+\Delta k} \\ U_{2,k+\Delta k} \end{bmatrix} = \begin{bmatrix} 1 & 0 & 0 \\ 0 & e^{-\frac{\Delta k}{\tau_1}} & 0 \\ 0 & 0 & e^{-\frac{\Delta k}{\tau_2}} \end{bmatrix} \begin{bmatrix} SOC_k \\ U_{1,k} \\ U_{2,k} \end{bmatrix} + \begin{bmatrix} -\frac{\eta\Delta k}{Q_0} \\ R_1(1-e^{-\frac{\Delta k}{\tau_1}}) \\ R_2(1-e^{-\frac{\Delta k}{\tau_2}}) \end{bmatrix} I(k) + \omega(k) \tag{3}$$

The discrete initial state equation can be obtained as shown in Eq. (4).

$$U_{L,k} = U_{oc,k} - R_{1,k}I(k) + \begin{bmatrix} 0 & -1 & -1 \end{bmatrix} \begin{bmatrix} SOC_{k+\Delta k} \\ U_{1,k+\Delta k} \\ U_{2,k+\Delta k} \end{bmatrix} + v(k) \tag{4}$$

wherein Δk is the sampling time interval, $\tau_1 = R_1C_1$ and $\tau_2 = R_2C_2$. w is the state error, and v is the measurement error, which are the zero-mean white noises of the covariance matrices Q and R, respectively.

Parameter identification

The estimation of the state of charge largely depends on the equivalent model established for the characteristics of the battery [26]. In order to improve the accuracy of the parameter identification of the battery model, it is necessary to adopt an

appropriate parameter identification method. Parameter identification methods are divided into online and offline parameter identification methods. For offline parameter identification methods [27], the internal parameters of the battery are obtained by fitting the battery characteristics curve. The parameters are solidified in the battery model and cannot change with the aging of the battery, temperature, and other factors [28, 29]. The online parameter identification algorithm can identify the time-varying parameters online, which can effectively solve the problem of offline parameter identification [30, 31].

Forgetting factor recursive least square algorithm

The forgetting factor recursive least square (FFRLS) algorithm is a commonly used parameter identification method [32]. The forgetting factor is introduced to reduce the influence of previous data on the current calculation and avoid the problem of data saturation [33]. The principle of the forgetting factor recursive least square algorithm is to use the identification results of the previous moment and the system input and output values of the current moment to recursively deduce the system parameters that need to be identified at the current moment [34, 35]. When the for- getting factor recursive least square algorithm is used for parameter identification, the expression of terminal voltage prediction error is expressed as shown in Eq. (5).

$$e_0(k) = y(k) - \phi(k)\hat{\theta}(k-1) \tag{5}$$

wherein $\gamma(k)$ is the true voltage at time k and $\bar{\phi}(k)\theta\Lambda(k-1)$ is the is predict the voltage at time k.

Improved proportional control forgetting factor recursive least square algorithm

Since the model accuracy is determined by the real voltage and the real-time output voltage error value of the model and considering the non-eliminating steady-state error under dynamic conditions, a proportional control link is added based on the forgetting factor recursive least square algorithm to reduce the steady-state error. The corrected error is brought into the system to obtain a more accurate real-time output voltage of the model, and then more accurate model parameters are obtained to improve the parameter identification accuracy. The system equation of the proportional control forgetting factor recursive least square (PCFFRLS) algorithm is shown in Eqs. (6) to (9).

The identified parameter expression is shown in Eq. (6).

$$\hat{\theta}(k) = \hat{\theta}(k-1) + K(k)\left[y(k) - \phi(k)\hat{\theta}(k-1)\right] \tag{6}$$

wherein $\theta(k)$ is the estimated value of identification parameters at the current time, $\phi(k)$ is the system input, and $\gamma(k)$ is the system output.

The algorithmic gain matrix is shown in Eq. (7).

$$K(k) = P(k-1)\phi(k)\left[\lambda + \phi^T(k)P(k-1)\phi(k)\right]^{-1} \tag{7}$$

wherein λ is the forgetting factor. The forgetting factor is the weight ratio of the previous moment to the next moment. When the newly added data cannot correct the identification results normally, it is necessary to reduce the weight of the old data and increase the role of the new data. The algorithm has the ability to respond quickly to the change in input process characteristics. The value range of $,1$ is $0 < \lambda \leq 1$. In this paper, $L = 0.99$.

The covariance matrix is shown in Eq. (8).

$$P(k) = \frac{1}{\lambda}\left[E - K(k)\phi^T(k)\right]P(k-1) \tag{8}$$

After adding the proportional control link, the system error expression is shown in Eq. (9).

$$e(k) = y(k) - \phi(k)\hat{\theta}(k-1) + P(y(k) - U_k) \tag{9}$$

wherein U_k is the real-time output voltage of the model at time k and P is the proportional gain coefficient. Properly increasing the proportional gain coefficient can ensure the tracking ability of the system to the given signal. When the proportional gain coefficient is too large, the stability of the system will deteriorate and even lead to system instability. After program code debugging, when the proportional gain coefficient is between 1 and 5%, the result is good. In this paper, $P = 0.004$.

OCV-SOC curve fitting

There is a certain mathematical relationship between the open circuit voltage (OCV) of lithium-ion batteries and the state of charge. The ternary lithium-ion battery with a rated capacity of 70Ah and an actual capacity of 62.76Ah was selected for the experiment. With BTS200-100–104 battery test equipment as the experimental platform, the lithium-ion battery was tested by HPPC [36]. The experimental steps were as follows: first, the battery was fully charged in a standard constant current and constant voltage manner [37]; the battery was left for 10 min; 1C was discharged for 10 s in a constant current manner; hold for 40 s; charge at a constant current of 1C for 10 s; shelve. The interval between 10 SOC pulse cycles with SOC of 1, 0.9, 0.8… 0.2, 0.1 is 40 min.

Through the analysis of state of charge and corresponding open circuit voltage [38, 39] based on the data obtained from HPPC experiment, the specific values of the open-circuit voltage in the equivalent circuit model used when the state of charge is in different stages are obtained. The SOC and OCV data under HPPC test are shown in Table 1.

Table 1 SOC and OCV data under HPPC test

SOC	OCV(V)
1	4.1892
0.9	4.0531
0.8	3.9388
0.7	3.8352
0.6	3.7236
0.5	3.6520
0.4	3.6166
0.3	3.5869
0.2	3.5258
0.1	3.4523

The functional relationship between SOC and OCV can be obtained by the data fitting method, and the positive correlation between SOC and OCV can be roughly obtained by experimental data. The power of the function is positively related to the fitting accuracy, but the higher the power, the greater the amount of calculation, which requires a balance between the accuracy of the fitting and the amount of calculation. Under this experimental condition, the curve is fitted by a sixth-order polynomial. The mathematical relationship between OCV and SOC is shown in Eq. (10).

$$\begin{aligned} OCV(S) = {} & 36.39S^6 - 116.2S^5 + 140.5S^4 - 79.27S^3 + \\ & 21.07S^2 - 1.854S + 3.514 \end{aligned} \tag{10}$$

The OCV-SOC fitting curve is shown in Fig. 2.

Fig. 2

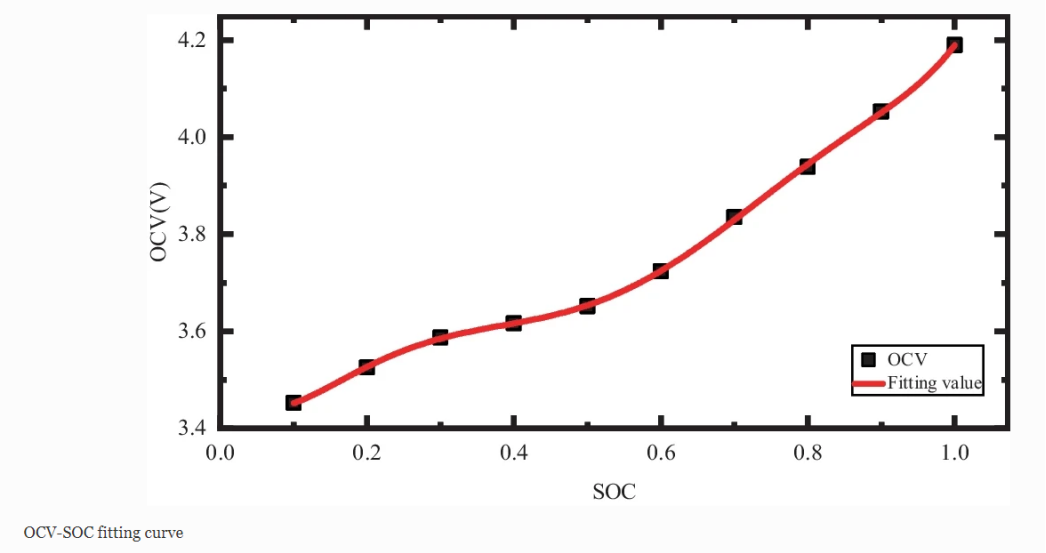

OCV-SOC fitting curve

When the order of fit is too low, the curve does not better reflect the relationship between SOC and OCV. When the order of fit is too high, oscillation will occur, which will affect the accuracy. Figure 2 shows that the sixth-order fitting curve can effectively reflect the relationship between SOC and OCV. Through this curve, the SOC of lithium-ion batteries can be calculated from OCV.

Extended Kalman filtering

Kalman filtering is a method suitable for working in linear state systems [40]. The principle of the Kalman filtering is to obtain the optimal estimation of the state variables at the current time of the system by using the estimates from the previous moment and the measurements from the current moment, including two steps of prediction and analysis [41, 42]. Because the Kalman filtering only considers the time domain and not the frequency domain, the estimation is simple and effective. Since the Kalman filtering is only applicable to linear systems, non-linear systems do not perform well. Therefore, in order to make a series of algorithms that can be used in the field of non-linear systems, after continuous research, some scholars have proposed the extended Kalman filtering algorithm [43, 44]. The extended Kalman filtering algorithm converts a non-linear system [45] into a linear system using a Taylor formula. The state space equation of the nonlinear discrete system is shown in Eq. (11).

$$\begin{cases} x_{k+1} = \mathrm{f}(x_k, u_k) + w_k \\ y_k = g(x_k, u_k) + v_k \end{cases} \tag{11}$$

wherein x_k is the value at time k of the system, y_k is the measured value at time k of the system, u_k is input. w_k is the state error, and v_k is the measurement error, which are the zero-mean white noises.

The state vector of the system is shown in Eq. (12).

$$\begin{cases} x_k = (SOC_k, U_{1,k}, U_{2,k})^T \\ u_k = I_{t,k} \end{cases} \tag{12}$$

Combining Eqs. (3), (4), and (11) can calculate (13).

$$\begin{cases} f(x_k,u_k)=\begin{bmatrix}1 & 0 & 0\\ 0 & e^{-\frac{\Delta t}{\tau_1}} & 0\\ 0 & 0 & e^{-\frac{\Delta t}{\tau_2}}\end{bmatrix}x_k+\begin{bmatrix}-\eta\frac{\Delta t}{C}\\ R_1(1-e^{-\frac{\Delta t}{\tau_1}})\\ R_2(1-e^{-\frac{\Delta t}{\tau_2}})\end{bmatrix}u_k \\ g(x_k,u_k)=U_{ocv}(x_k[1])-i_kR_0-x_k[2]-x_k[3]\end{cases} \tag{13}$$

To simplify the above equations, the simplified equation is shown in Eq. (14).

$$\begin{cases} \hat{A}_k=\begin{bmatrix}1 & 0 & 0\\ 0 & e^{-\frac{\Delta t}{\tau_1}} & 0\\ 0 & 0 & e^{-\frac{\Delta t}{\tau_2}}\end{bmatrix} \\ \hat{B}_k=\begin{bmatrix}-\eta\frac{\Delta t}{C} & R_1(1-e^{-\frac{\Delta t}{\tau_1}}) & R_2(1-e^{-\frac{\Delta t}{\tau_2}})\end{bmatrix}^T \\ \hat{C}_k=\left[\frac{dU_{ocv}}{SOC},-1,-1\right] \\ \hat{D}_k=-R_0\end{cases} \tag{14}$$

The specific process of the extended Kalman filtering algorithm is:

1. Initialization:

$$\begin{cases} \hat{x}_0=E(x_0) \\ \hat{P}_0=E[(x_0-\hat{x}_0^+)(x_0-\hat{x}_0^+)^T]\end{cases} \tag{15}$$

2. Updating state variables:

$$\hat{x}_k^-=f(\hat{x}_{k-1}^+,u_{k-1}) \tag{16}$$

3. Updating mean square estimate:

$$P_k^-=\hat{A}_{k-1}P_{k-1}^+\hat{A}_{k-1}^T+Q_k \tag{17}$$

4. Calculating Kalman gain:

$$L_k^-=P_k^-\hat{C}_k^T(\hat{C}_kP_k^-\hat{C}_k^T+R_k)^{-1} \tag{18}$$

5. Optimal estimation of state variables:

$$\hat{x}_k^+=\hat{x}_k^-+G_k[y_k-g(\hat{x}_k^-u_k)] \tag{19}$$

6. Optimal estimation of mean square estimation error:

$$P_k^+=(1-G_k\hat{C}_k)P_k^- \tag{20}$$

7. Determine whether k can be stopped. If not, add 1 to k and return to step (2) until it stops.

Adaptive extended Kalman filtering

In order to reduce the error caused by the extended Kalman filtering algorithm ignoring the influence of noise in the actual process [46, 47], the adaptive extended Kalman filtering algorithm [48] estimates and corrects the process and measurement noise of the system by comparing the final estimates with the predictions. At the same time, process noise and measurement noise of the system is estimated and corrected, and average estimation and covariance are adjusted to reduce

the impact of noise on state-of-charge estimation, so as to obtain higher accuracy of state-of-charge estimation results.

The calculation process of noise variable is shown in Eqs. (21) to (24).

$$q_{k+1} = \frac{1}{k+1} G \sum_{i=0}^{k} (\hat{x}_{k+1} - A\hat{x}_k - B\hat{u}_k) \tag{21}$$

$$Q_{k+1} = \frac{1}{k+1} G \sum_{i=0}^{k} (K_{k+1}\tilde{y}_{k+1} y_{k+1}^T K_{k+1}^T + \tilde{P}_{k+1/k} - A\tilde{P}_{k+1/k}A^T) G^T \tag{22}$$

$$r_{k+1} = \frac{1}{k+1} \sum_{i=0}^{k} (y_{k+1} - C\hat{x}_{k+1}) \tag{23}$$

$$R_{k+1} = \frac{1}{k+1} \sum_{i=0}^{k} (\overline{y}_{k+1}\overline{y}_{k+1}^T - C\tilde{P}_{k+1/k}C^T) \tag{24}$$

In Eq. (21), q_{k+1} is the system state noise, $\hat{x_k}$ is the state of the system at time k, A is the system state transition matrix, and B is the control matrix. In Eq. (22), Q_{k+1} is the covariance matrix of system state noise, y_{k+1} is the state observation measurement, and G is the noise driven matrix. $\tilde{P}_{k+1/k}$ is the error covariance matrix of initial prediction. In Eq. (23), r_{k+1} is the system observation noise, and C is the system measurement matrix. In Eq. (24), R_{k+1} is the covariance matrix of system observation noise.

Due to the accidental error in the measurement, in order to more accurately characterize the impact of noise, this paper uses weighting coefficients [49, 50] to reduce the weight of noise at time k, and its calculation formula is shown in Eq. (25).

$$d_k = \frac{1-b}{1-b^{k+1}} \tag{25}$$

wherein b is the forgetting factor. In practical applications, the smaller the value of b, the smaller the impact of the previous moment. However, a small value of b will cause the estimated noise to fluctuate. If the value of b is too large, the impact of the previous moment will be too large. Therefore, the value can be taken according to the specific situation. In this paper, $b = 0.98$.

After correction, the noise matrix calculation formula is shown in Eqs. (26) to (29).

$$q_{k+1} = (1-d_k)q_k + d_k G(\hat{x}_{k+1} - A\hat{x}_k - B\hat{u}_k) \tag{26}$$

$$Q_{k+1} = (1-d_k)Q_k + d_k G(K_{k+1}\tilde{y}_{k+1} y_{k+1}^T K_{k+1}^T + \tilde{P}_{k+1/k} - A\tilde{P}_{k+1/k}A^T) G^T \tag{27}$$

$$r_{k+1} = (1-d_k)r_k + d_k(y_{k+1} - C\hat{x}_{k+1} - Du_{k+1}) \tag{28}$$

$$R_{k+1} = (1-d_k)R_k + d_k(\tilde{y}_{k+1}\tilde{y}_{k+1}^T - CP_{k+1/k}C^T) \tag{29}$$

The specific process of the adaptive extended Kalman filtering algorithm is:

1. Calculating the system state and error covariance matrix at time k:

$$\hat{x}_{k+1/k} = A\hat{x}_k + Bu_k + q_k \tag{30}$$

$$\tilde{P}_{k+1/k} = AP_kA^T + Q_k \tag{31}$$

2. Calculating the Kalman gain:

$$K_k = \frac{\tilde{P}_{k+1/k}C^T}{C\tilde{P}_{k+1/k}C^T + R_k} \tag{32}$$

wherein R_k is the measurement noise, $C = \left[\frac{\partial U_{oc}}{\partial SOC} \quad -1 \quad -1\right]$.

3. Calculating the system error covariance matrix at $k+1$ time:

$$\tilde{y}_{k+1} = y_{k+1} - (C\hat{x}_{k+1/k} + Du_k) - r_k \tag{33}$$

$$\hat{x}_{k+1} = \hat{x}_{k+1/k} + K_k\tilde{y}_{k+1} \tag{34}$$

$$P_{k+1} = (E - K_kC)\tilde{P}_{k+1/k} \tag{35}$$

4. Updating noise q_k, r_k, Q_k, R_k, as shown in Eqs. (26) to (29).

Monte Carlo method

The Monte Carlo method is also called the statistical simulation method. It is a numerical simulation method that takes probability phenomenon as the research object. It is the calculation method of estimating an unknown characteristic quantity by obtaining statistical value according to the sampling survey method. This method is suitable for computing and simulating discrete systems. The basic approach of Monte Carlo is to estimate the probability through a large number of repeated tests and statistical frequency, so as to get the solution to the problem. In general, the characteristic of the Monte Carlo method is that the more samples, the more approximate to the optimal solution, but never the optimal solution. The problems with statistical properties can be solved directly, and the continuous problems need not be discretized.

There is noise in the system, which is reduced through an adaptive process. During the calculation, the SOC value is related to the noise. Through the Monte Carlo method, the real SOC is resampled many times, and its results are averaged. It is considered that the SOC is the optimal solution, that is, the real value of SOC. In the process of SOC estimation, to reduce the impact of random noise on the estimation results, the SOC at each time is sampled 1000 times of repeated estimation. Finally, calculate the average value of 1000 samples at each time as the final approximate estimate of SOC at that time. The approximate estimate of SOC at each time is shown in Eq. (36).

$$\bar{\hat{x}}_k = \frac{\sum_{j=1}^{1000} x_k^{(j)}}{1000} \tag{36}$$

wherein $\bar{\hat{x}_k}$ is the estimated value of SOC at time k.

Because the AEKF algorithm considers the influence of real noise, its adaptive link reduces the influence of noise in the SOC estimation process, and the Monte Carlo method can further reduce the influence of random noise on the estimation results. At the same time, it also reduces the influence of the inaccuracy of the prior estimation on the posterior estimation. Using the improved proportional control forgetting factor recursive least square algorithm for parameter identification can improve the accuracy of identification results. But due to the existence of system noise, it will still have an impact on the accuracy of state-of-charge estimation, while the Monte Carlo adaptive extended Kalman filtering algorithm can effectively improve the accuracy of state-of-charge estimation due to its adaptive filtering method and strong ability to suppress noise. The framework diagram of lithium-ion battery state-of-charge estimation using two algorithms is shown in Fig. 3.

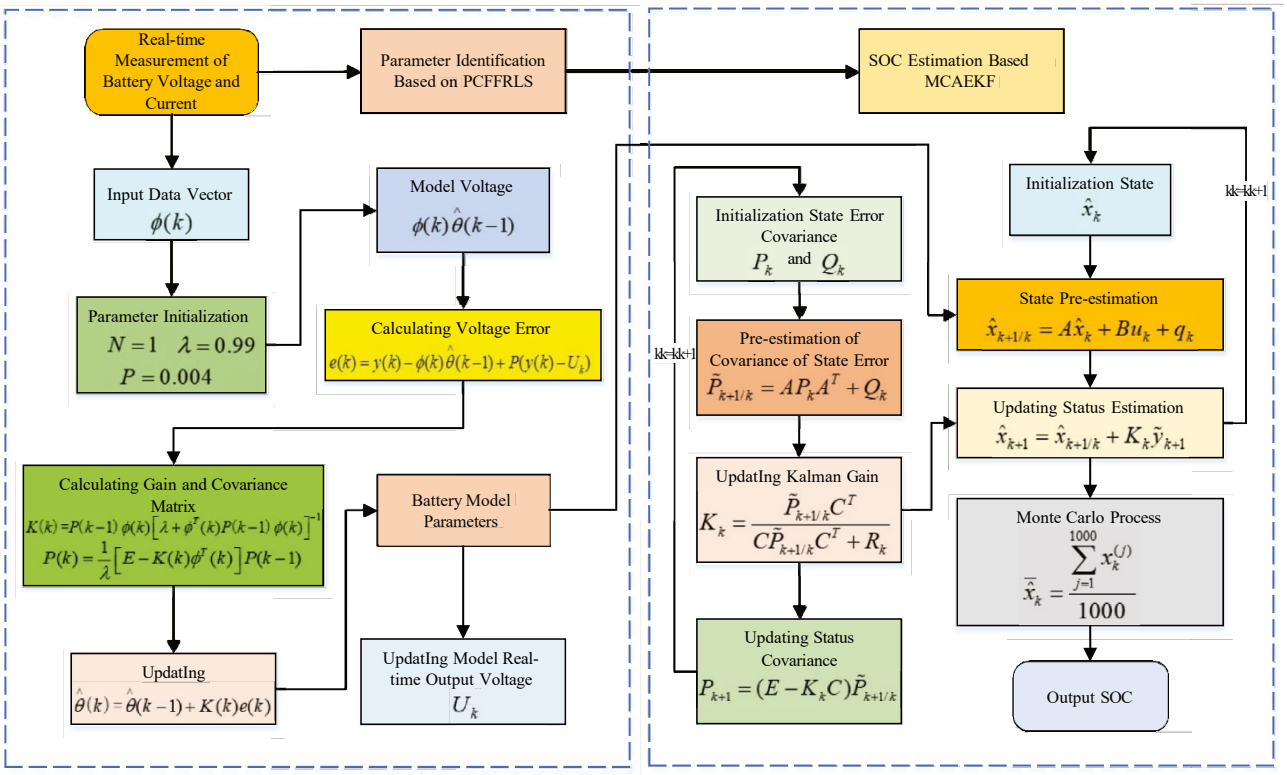

Fig. 3 SOC estimation framework of PCFFRLS-MCAEKF

First, the voltage, current, and other data of lithium-ion batteries under working conditions are measured through experiments, and the battery model parameters are identified based on an improved forgetting factor recursive least square algorithm to obtain the relevant parameters of the model. Then the parameters are transferred to the adaptive extended Kalman filtering algorithm, and the system state, gain matrix, and covariance matrix are calculated by combining the voltage and current data to estimate the state of charge. Finally, the final SOC estimate is obtained by updating the SOC estimate through the Monte Carlo process.

Experimental verification

In order to verify the superiority of PCFFRLS-MCAEKF algorithm, this paper uses FFRLS and PCFFRLS algorithms to determine lithium-ion battery parameters based on the second-order RC equivalent circuit model. Verify the accuracy of parameter identification and state-of-charge estimation under HPPC and BBDST working conditions.

HPPC condition

The voltage comparison diagram of different parameter identification algorithms under HPPC working conditions is shown in Fig. 4.

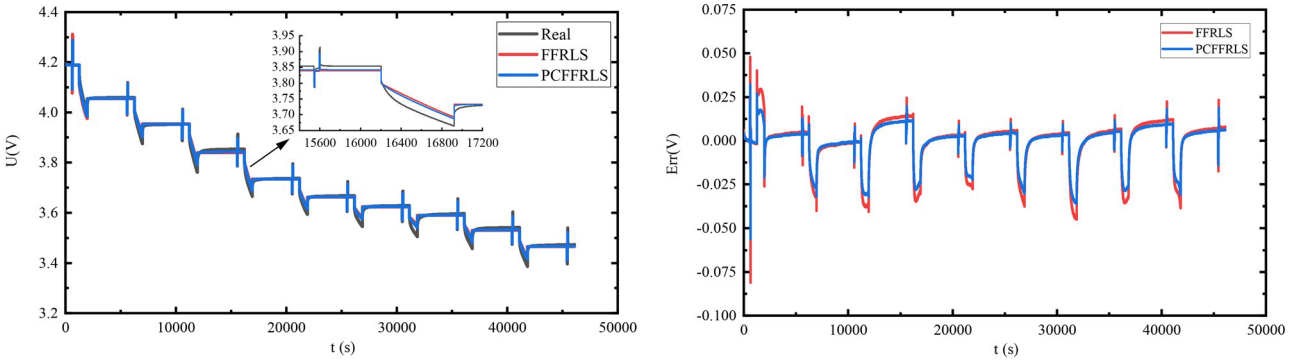

(a) Real voltage and model output voltage

(b) Voltage simulation error

Fig. 4 Voltage comparison under HPPC working condition

Comparing the model output voltage of FFRLS and PCF- FRLS, the model output voltage of PCFFRLS is closer to the real value. At the initial stage, the PCFFRLS algorithm has a large error, which is caused by the initial parameter setting, but it is still better than the FFRLS algorithm. With the iteration of the algorithm, its error gradually decreases. In the intermediate stage, the PCFFRLS algorithm corrects the model's real-time output voltage to make it closer to the true voltage by reducing the current time error due to the unavoidable influence of the steady-state error in the actual situation. Root mean square error and mean absolute error are selected as evaluation indexes in this paper. The error comparison of different parameter identification algorithms is shown in Table 2.

Table 2 Error comparison

Algorithm	RMSE/V	MAE/V
FFRLS	0.01295	0.00023
PCFFRLS	0.01031	0.00011

According to the data comparison in Table 2, under HPPC condition, the mean square root error and mean absolute error of PCFFRLS algorithm are smaller than FFRLS algorithm. This shows that PCFFRLS algorithm has higher accuracy and stability, and can effectively improve the accuracy of parameter identification.

The model parameters identified by FFRLS and PCF-FRLS algorithms were replaced with HPPC condition data, and SOC accuracy was verified using EKF, AEKF, and MCAEKF algorithms. The comparison of SOC estimation results and the comparison of SOC estimation errors of different algorithms are shown in Fig. 5.

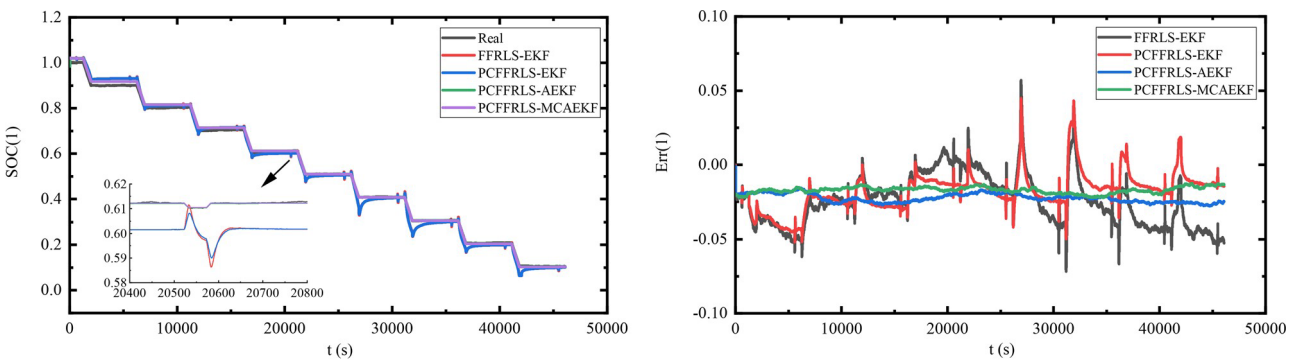

(a) SOC Estimation Results

(b) SOC Estimation Error

Fig. 5 SOC comparison under HPPC working condition

Compared with the SOC estimation results of different algorithms, AEKF algorithm is more stable and closer to the true value than EKF algorithm. This is because the EKF algorithm ignores the noise in the discharge process, and the cumulative error of noise makes the SOC estimation error increase. MCAEKF algorithm has smaller error than AEKF algorithm, and its SOC estimation accuracy is higher. In the process of lithium battery SOC estimation, MCAEKF algorithm obtains the expected SOC estimation value by continuously correcting the noise through 1000 resamples of the real noise, reducing the impact of noise on the estimation accuracy. The SOC estimation error of the PCFFRLS-EKF algorithm is smaller than that of the FFRLS-EKF algorithm, because the PCFFRLS algorithm has better parameter identification results and higher model parameter accuracy.

Table 3 shows the comparison of SOC estimation errors of different algorithms. Under HPPC working conditions, the root mean square error and average absolute error of PCFFRLS-MCAEKF algorithm are the minimum. The root mean square error of PCFFRLS-MCAEKF algorithm is reduced by 1.275%, 0.687%, and 0.549% compared with FFRLS-EKF, PCFFRLS-EKF, and PCFFRLS-AEKF algorithm, and the average absolute error is reduced by 0.71%, 0.537%, and 0.11%. It can be seen that PCFFRLS-MCAEKF algorithm can estimate the state of charge of the lithium-ion batteries more accurately.

Table 3 Comparison of SOC estimation errors of different algorithms of different parameter identification algorithms

Algorithm	RMSE	MAE
FFRLS-EKF	0.02997	0.02421
PCFFRLS-EKF	0.02409	0.02248
PCFFRLS-AEKF	0.02271	0.01821
PCFFRLS-MCAEKF	0.01722	0.01711

BBDST condition

The voltage comparison diagram of different parameter identification algorithms under BBDST working conditions is shown in Fig. 6. The error comparison of different parameter identification algorithms is shown in Table 4.

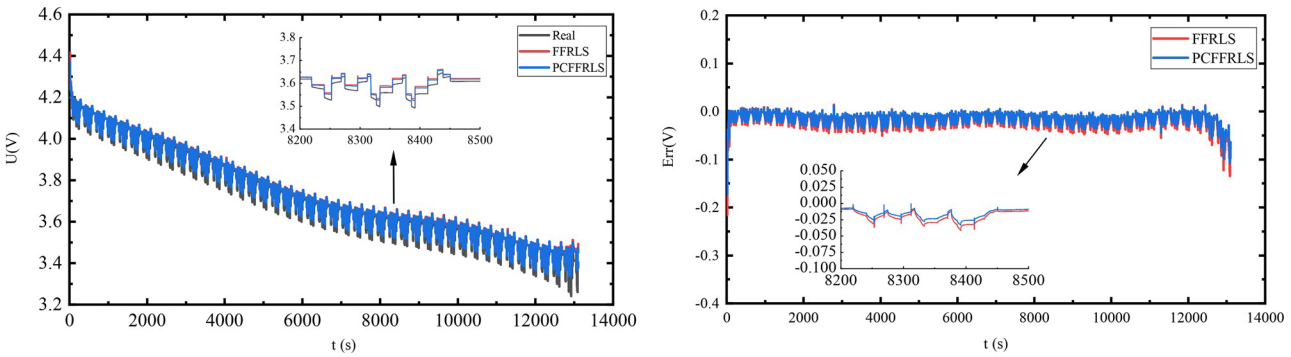

(a) Real voltage and model output voltage

(b) Voltage simulation error

Fig. 6 Voltage comparison under BBDST working condition

Table 4 Error comparison of different parameter identification algorithms

Algorithm	RMSE/V	MAE/V
FFRLS	0.02479	0.01995
PCFFRLS	0.01983	0.01596

According to the data comparison in Table 4, under BBDST condition, the mean square root error and mean absolute error of PCFFRLS algorithm are smaller than FFRLS algorithm. The comparison of SOC estimation results and the comparison of SOC estimation errors of different algorithms are shown in Fig. 7.

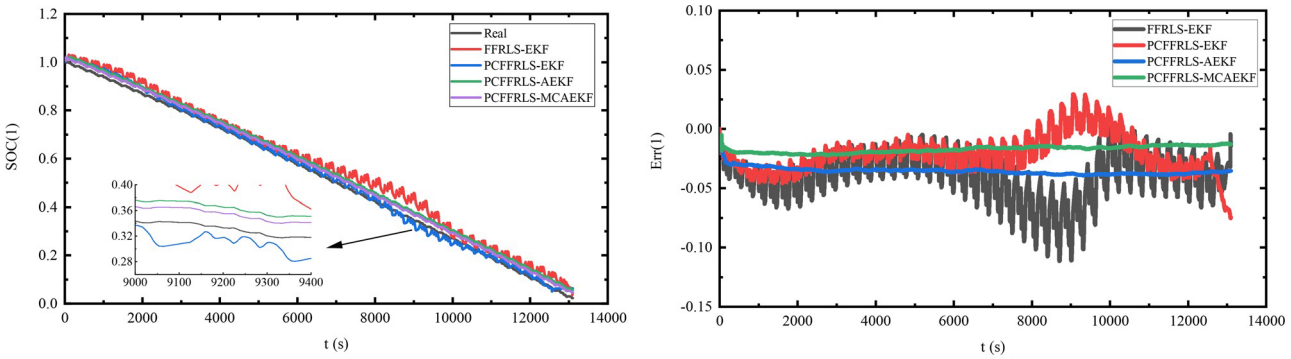

(a) SOC Estimation Results **(b)** SOC Estimation Error

Fig. 7 SOC comparison under BBDST working condition

Table 5 shows the comparison of SOC estimation errors of different algorithms. Under BBDST working conditions, due to the influence of random noise in the actual process, the error of EKF and AEKF algorithms is large. However, the influence of random noise on the estimation result is reduced through the Monte Carlo process, which shows that the Monte Carlo process can improve the accuracy of SOC estimation.

Table 5 Comparison of SOC estimation errors of different algorithms

Algorithm	RMSE	MAE
FFRLS-EKF	0.04445	0.03937
PCFFRLS-EKF	0.02643	0.02448
PCFFRLS-AEKF	0.03569	0.02823
PCFFRLS-MCAEKF	0.01751	0.01711

According to the comparison data, the root mean square error and average absolute error of the PCFFRLS-MCAEKF algorithm are the minimum. The SOC estimation result of the PCFFRLS-MCAEKF algorithm is closer to the real SOC, which is consistent with the result obtained under HPPC working conditions. It can be seen that the PCFFRLS- MCAEKF algorithm can estimate the state of charge of the lithium-ion batteries more accurately.

Conclusion

In view of the problem that the system has inevitable steady-state error under dynamic conditions, this paper added a proportional control link based on the forgetting factor recursive least square algorithm and proposed an improved proportional control forgetting factor recursive least square algorithm. This method reduces the steady-state error through a proportional control link. The corrected errors are fed back to the system to obtain a more accurate model real-time output voltage, which leads to more accurate model parameters. This method improves the accuracy of parameter identification. Based on the second-order RC equivalent circuit model, FFRLS and PCFFRLS algorithms are used for parameter identification, respectively, and the identification results are transferred to EKF, AEKF, and MCAEKF algorithms for high-precision SOC estimation. The Monte Carlo method can further reduce the influence of random noise on the estimation results. Through simulation comparison, under HPPC and BBDST conditions, the parameter identification accuracy of the PCFFRLS algorithm is higher than that of the FFRLS algorithm. The PCFFRLS-MCAEKF algorithm has higher SOC estimation accuracy than FFRLS- EKF, PCFFRLS-EKF, and PCFFRLS-AEKF algorithms. PCFFRLS algorithm improves the accuracy of parameter identification, and the PCFFRLS-MCAEKF algorithm improves the accuracy and robustness of state-of-charge estimation for lithium-ion batteries.

Funding The work was supported by the National Natural Science Foundation of China (No.62173281,61801407).

References

1. Feng J et al (2021) Online SOC estimation of a lithium-ion battery based on FFRLS and AEKF. Energy Storage Science and Technology 10(1):242–249
2. Wang H, Zheng Y, Yu Y (2021) Lithium iron phosphate battery SOC estimation based on the least square online identification of dynamic optimal forgetting factor. Automobile Technology 10:23–29
3. Sun J et al (2022) State of charge estimation for lithium-ion battery based on FFRLS-EKF joint algorithm. Automot Eng 44(4):505–513
4. Li Y et al (2020) Comparative study of the influence of open circuit voltage tests on state of charge online estimation for lithium-ion batteries. IEEE Access 8:17535–17547
5. Xiong X et al (2020) A novel practical state of charge estimation method: an adaptive improved ampere-hour method based on composite correction factor. Int J Energy Res 44(14):11385–11404
6. Ren Z et al (2021) A comparative study of the influence of different open circuit voltage tests on model-based state of charge estimation for lithium-ion batteries. Int J Energy Res 45(9):13692–13711
7. Beelen H, Bergveld HJ, Donkers MCF (2021) Joint estimation of battery parameters and state of charge using an extended Kalman filter: a single-parameter tuning approach. IEEE Trans Control Syst Technol 29(3):1087–1101
8. Jemmali S, Manai B, Hamouda M (2022) Pure hardware design and implementation on FPGA of an EKF based accelerated SoC estimator for a lithium-ion battery in electric vehicles. IET Power Electronics 15(11):1004–1015
9. Jin YZ, Su CL, Luo SC (2022) Improved algorithm based on AEKF for state of charge estimation of lithium-ion battery. Int J Automot Technol 23(4):1003–1011
10. Gu TY et al (2022) The modified multi-innovation adaptive EKF algorithm for identifying battery SOC. Ionics 28(8):3877–3891
11. Liu QH, Yu QQ (2022) The lithium battery SOC estimation on square root unscented Kalman filter. Energy Rep 8:286–294
12. Wang LM et al (2022) State of charge estimation of lithium- ion based on VFFRLS-noise adaptive CKF algorithm. Ind Eng Chem Res 61(22):7489–7503
13. Xu H et al (2022) A novel Drosophila-back propagation method for the lithium-ion battery state of charge estimation adaptive to complex working conditions. Int J Energy Res 46(11):15864–15880
14. Saha P, Dey S, Khanra M (2020) Modeling and state-of-charge estimation of supercapacitor considering leakage effect. IEEE Trans Industr Electron 67(1):350–357
15. Zhu L et al (2021) Research on a battery SOC prediction method based on the RLS-DLUKF algorithm. Energy Storage Science and Technology 10(3):1137–1144
16. Fu SY et al (2022) Study of impacts of parameters identification methods on model-based state estimation for LiFePO4 battery. Ionics 28(7):3321–3339
17. Du XH et al (2022) An information appraisal procedure: endows reliable online parameter identification to lithium-ion battery model. IEEE Trans Industr Electron 69(6):5889–5899
18. Sun P et al (2021) Research on online parameter identification and SOC estimation of battery under dynamic conditions. Journal of Electronic Measurement and Instrument 35(1):10–17
19. Sylvestrin GR, Scherer HF, Ando OH (2022) Experimental validation of state of charge estimation by extended Kalman filter and modified Coulomb counting. IEEE Lat Am Trans 20(11):2395–2403
20. Naseri F et al (2022) An enhanced equivalent circuit model with real-time parameter identification for battery state-of-charge estimation. IEEE Trans Industr Electron 69(4):3743–3751
21. Takyi-Aninakwa P et al (2022) A strong tracking adaptive fading-extended Kalman filter for the state of charge estimation of lithium- ion batteries. Int J Energy Res 46(12):16427–16444
22. Tang AH et al (2022) Lithium-ion battery state-of-charge estimation of an order-reduced physics-based model in electric vehicles considering erroneous initialization. Int J Energy Res 46(3):3529–3538
23. Li L et al (2020) A novel online parameter identification algorithm for fractional-order equivalent circuit model of lithium-ion batteries. Int J Electrochem Sci 15(7):6863–6879
24. Qays MO et al (2022) Recent progress and future trends on the state of charge estimation methods to improve battery-storage efficiency: a review. Csee Journal of Power And Energy Systems 8(1):105–114
25. Adaikkappan M, Sathiyamoorthy N (2022) Modeling, state of charge estimation, and charging of lithium-ion battery in electric vehicle: A review. Int J Energy Res 46(3):2141–2165
26. Li JB et al (2021) State estimation of lithium polymer battery based on Kalman filter. Ionics 27(9):3909–3918
27. Hu L et al (2022) Performance evaluation strategy for battery pack of electric vehicles: online estimation and offline evaluation. Energy Rep 8:774–784
28. Chen PY et al (2022) Evaluation of various offline and online ECM parameter identification methods of lithium-ion batteries in underwater vehicles. ACS Omega 7(34):30504–30518
29. Kwak M et al (2020) Parameter identification and SOC estimation of a battery under the hysteresis effect. IEEE Trans Industr Electron 67(11):9758–9767
30. van der Meer GH et al (2021) Practical guidelines to build sense of community in online medical education. Med Educ 55(8):925–932
31. Ouyang Q, Chen J, Zheng J (2020) State-of-charge observer design for batteries with online model parameter identification: a robust approach. IEEE Trans Power Electron 35(6):5820–5831
32. Liu YY et al (2022) A novel adaptive H-infinity filtering method for the accurate SOC estimation of lithium-ion batteries based on optimal forgetting factor selection. Int J Circuit Theory Appl 50(10):3372–3386
33. Wang J, Zhang Z, Li P (2021) State of charge estimation for lithium-ion battery based on adaptive recursive weighted least squares and extended Kalman filter algorithm. Automobile Technology 10:16–22

34. Miao H et al (2021) A novel online model parameters identification method with anti-interference characteristics for lithium-ion batteries. Int J Energy Res 45(6):9502–9517
35. Qu DW et al (2022) State of charge estimation for the vanadium redox flow battery based on extended Kalman filter using modified parameter identification. Energy Sources Part A-Recovery Utilization and Environmental Effects 44(4):9747–9763
36. Lai X et al (2021) An overall estimation of state-of-charge based on SOC-OCV optimization curve and EKF for lithium-ion battery. Automot Eng 43(1):19–26
37. Huang XR et al (2022) Effect of pulsed current on charging performance of lithium-ion batteries. IEEE Trans Industr Electron 69(10):10144–10153
38. He L et al (2020) State of charge estimation by finite difference extended Kalman filter with HPPC parameters identification. Science China-Technological Sciences 63(3):410–421
39. Wang QT, Qi W (2020) New SOC estimation method under multi-temperature conditions based on parametric-estimation OCV. J Power Electron 20(2):614–623
40. Zhou J et al (2021) Research on the SOC estimation algorithm of combining sliding mode observer with extended Kalman fil- ter. Proceedings of the Chinese Society of Electrical Engineering 41(2):692–702
41. Al-Gabalawy M et al (2021) State of charge estimation of a Li-ion battery based on extended Kalman filtering and sensor bias. Int J Energy Res 45(5):6708–6726
42. Li WQ et al (2020) The multi-innovation extended Kalman filter algorithm for battery SOC estimation. Ionics 26(12):6145–6156
43. Gholizadeh M, Yazdizadeh A (2020) Systematic mixed adaptive observer and EKF approach to estimate SOC and SOH of lithium-ion battery. IET Electrical Systems in Transportation 10(2):135–143
44. Yu Y, Zheng Y (2021) SOC Estimation of lithium batteries based on improved recursive least squares method. Control Engineering of China 28(9):1759–1764
45. Wu C et al (2021) State of charge estimation of lithium-ion batteries based on maximum correlation-entropy criterion extended Kalman filtering algorithm. Transactions of China Electrotechnical Society 36(24):5165–5175
46. He ZC et al (2020) A method of state-of-charge estimation for EV power lithium-ion battery using a novel adaptive extended Kalman filter. IEEE Trans Veh Technol 69(12):14618–14630
47. Ali MU et al (2022) An adaptive state of charge estimator for lithium-ion batteries. Energy Science & Engineering 10(7):2333–2347
48. Xu JY, Wang DQ (2022) A dual-rate sampled multiple innovation adaptive extended Kalman filter algorithm for state of charge estimation. Int J Energy Res 46(13):18796–18808
49. Huang C et al (2021) State of charge estimation of li-ion batteries based on the noise-adaptive interacting multiple model. Energy Rep 7:8152–8161
50. Xia L et al (2021) Research on SOC estimation method of ternary lithium battery based on AEKF algorithm. Control Engineering of China 28(4):730–735